

# Microbially mediated release of As from Mekong

## Delta peat sediment

Maria P. Asta<sup>1\*</sup>, Yuheng Wang<sup>1</sup>, Manon Frutschi<sup>1</sup>, Karen Viacava<sup>1</sup>, Luca Loreggian<sup>1</sup>,  
Pierre Le Pape<sup>2</sup>, Phu Le Vo<sup>3</sup>, Ana María Fernández<sup>4</sup>, Guillaume Morin<sup>2</sup>  
and Rizlan Bernier-Latmani<sup>1</sup>

<sup>1</sup>École Polytechnique Fédérale de Lausanne (EPFL), Environmental Microbiology Laboratory (EML), Station 6, CH-1015 Lausanne, Switzerland

<sup>2</sup>Centre National de la Recherche Scientifique (CNRS) – Université Pierre et Marie Curie (UPMC Paris 6), Institut de Minéralogie, de Physique des Matériaux et de Cosmochimie (IMPMC, CNRS-UPMC-IRD-MNHN UMR 7590), Campus Jussieu, 4 place Jussieu, 75005 Paris, France

<sup>3</sup>Ho Chi Minh City University of Technology - VNU HCM, Faculty of Environment & Natural Resources, 268 Ly Thuong Kiet st., Dist. 10, Ho Chi Minh City, Vietnam

<sup>4</sup>Centro de Investigaciones Energéticas, Medioambientales y Tecnológicas (CIEMAT), Dpto. Medio Ambiente, Madrid, Spain

\*correspondence to: [Maria-Pilar.Asta-Andres@univ-grenoble-alpes.fr](mailto:Maria-Pilar.Asta-Andres@univ-grenoble-alpes.fr); corresponding author present address: Univ. Grenoble Alpes, Univ. Savoie Mont Blanc, CNRS, IRD, IFSTTAR, ISTerre, 38000 Grenoble, France

### **Supporting Information:**

Pages: 23

Additional Methods

Figures S1 to S6

Tables S1 to S7

Supporting References

## Methods

**Analysis of sediment chemistry.** Three sampling trips were carried out in January 2015, October 2016 and December 2017 in the Mekong Delta in Vietnam (Fig. S1). Once in the laboratory, a portion of each core was dried under vacuum using a desiccator in an anoxic chamber for a few days and then ground in an agate mortar and homogenized to a fine powder that was then stored in sealed serum bottles until analysis or use in the experiments. The bulk chemical composition of the sediment samples was analyzed with a PANalytical<sup>®</sup> Axios-mAX X-ray fluorescence (XRF) spectrometer using wax fused pellets for both major and trace elements. The detection limits were 0.01 wt.% for major elements and 1 to 5 ppm for trace elements. The accuracies of the analyses were assessed by analysis of standard reference materials. Sediment total organic carbon (TOC) content was measured in dried homogenized samples with a Shimadzu<sup>®</sup> TOC-V CPH/CPN analyzer at Faculty of Geosciences and Environment of the University of Lausanne.

**Porewater squeezing.** The porewater of the core samples was obtained by the squeezing technique at 1.5 MPa<sup>1</sup>. Squeezing is analogous to the natural process of consolidation, caused by the deposition of material during geological time, but at a greatly accelerated rate. The squeezing process involves the expulsion of interstitial fluid from the saturated argillaceous material being compressed.<sup>2</sup> In squeezing experiments, the volume of water extracted depends on the water content of the rock sample, the rock properties (e.g., dry density, the relative contents of easily-squeezed clays and of stiffer materials like quartz and calcite), and the experimental conditions, such as, the pressure applied, the duration time of squeezing and size of the squeezing cell.

At the Centro de Investigaciones Energéticas, Medioambientales y Tecnológicas (CIEMAT), the squeezing rig is similar to that developed by Peters et al.<sup>3</sup> and Entwisle and Reeder<sup>2</sup>. The squeezer was designed to allow one-dimensional compression of the sample

by means of an automatic hydraulic ram operating downwards, the squeezed water being expelled from the top and bottom of the cell into vacuum vials, especially prepared to maintain anoxic conditions. The compaction chamber is made of type AISI 329 stainless steel (due to its high tensile strength and resistance to corrosion) with an internal diameter of 70 mm. The compaction chamber is 250 mm high with 20 mm wall thickness and allows pressures up to 100 MPa.

The filtration system allows the extraction of interstitial water by drainage at the top and at the bottom of the sample. This system is comprised of a 0.5  $\mu\text{m}$  stainless steel AISI 316L porous disk (Cr 17.36%, Ni 11.4%, Mo 2.15%, Si 0.94%, Mn 0.17%, C 0.027%, S 0.011%, P 0.022%, Fe 66.92%) in contact with the sample. The liquid was collected through stainless steel tubes (1/16 inch) in a vacuum vial sealed by a septum. The whole system remained under ambient conditions (room temperature of about 25°C and ambient atmosphere). However, a sampling circuit was designed to collect the water under anoxic conditions.

Prior to squeezing, the core samples were prepared inside an anoxic glove bag flushed with Ar. The external outer part of the core was removed by using a knife in order to discard possible contaminating material. The sample was weighed and placed into the body of the cell, which was closed. The squeezing cell and the sampling tubings were sealed and connected to the sampling vial, closing the system inside the glove box.

After assembling the cell in the hydraulic press, a small stress of 0.5 MPa was initially applied to remove the remaining gas from the cell. Then, the vacuum vial was flushed again with Ar prior to starting the test to remove any remaining oxygen from the cell and the sample, preserving the system under anoxic conditions.

The applied stress was increased slowly and progressively up to the selected pressure, rather than in a single step. This avoids overconsolidation or collapse of the pore system. The selected pressure was that minimum exerted for collecting the first water aliquot and

allowing the chemical analysis. After the squeezed water was obtained at minimum pressure, the vial was removed, keeping the sample away from the atmosphere. The sample collected was filtered by 0.2  $\mu\text{m}$  inside an anoxic glove box ( $< 1\text{ppm O}_2$ ) and distributed in subsamples preserved appropriately according to the type of analysis and, then, stored in a refrigerator at 4°C until its chemical analysis.

**Porewater chemical analysis.** The porewater analysis were carried out at the Centro de Investigaciones Energéticas, Medioambientales y Tecnológicas (CIEMAT), except the ammonium, the iron and arsenic speciation and the sulfide analyses that were performed in the EPFL. The pH and alkalinity were measured immediately after sample collection. For the pH, a Metrohm 6.0224.100® combined glass pH micro-electrode with temperature compensation after calibration with standard buffer solutions of pH 2, 7 and 9 was used. The total alkalinity was determined with a specific Dynamic Equivalence point Titration (DET) method for analyzing samples of 1-2 mL. The instrumentation consists of a Metrohm 888 Titroprocessor equipped with a 5 mL burette and a 6.0224.100 Metrohm combined pH micro-electrode. The major and trace elements of porewater samples were analyzed by Inductively Coupled Plasma-Optical Emission Spectrometry (ICP-OES) in a Varian 735 ES spectrometer. Sodium and potassium were determined by atomic absorption spectrometry in an Agilent AA 240 FS spectrometer. Anions were analyzed by ion chromatography (Dionex ICS-2000). An ORION 901 microprocessor ion-analyzer, equipped with ion-selective electrodes, was employed for F and I determination. The DOC (dissolved organic carbon) was analyzed with a TOC-VCSH analyzer (Shimadzu Scientific Instruments, Kyoto, Japan). Sulfide and ferrous iron concentrations were determined spectrophotometrically on samples filtered through 0.2  $\mu\text{m}$  pore size filters by the methods described by Cline<sup>4</sup> and Stookey<sup>5</sup> using a UV-2501 PC spectrophotometer (Shimadzu, Japan). Arsenic speciation (As(III) and As(V)) was determined by HPLC/ICPMS (high-performance liquid

chromatography with inductively coupled plasma mass spectrometry) with a Perkin Elmer-Sciex Series 200 HPLC coupled to a Perkin Elmer-Sciex Elan DRC II ICPMS (Concord, Ontario, Canada). The error in the measurements is the standard deviation of at least three individual runs. The analytical error for major anions and cations (including necessary dilution steps) is  $\pm 5\%$ , except for K, Fe and alkalinity whose analytical error is  $\pm 10\%$ , and for DOC contents is  $\pm 1\%$ .

**Water chemistry analysis.** Water analyses from laboratory experiments were carried out at the Ecole Polytechnique Fédérale de Lausanne (EPFL) as follows. Concentrations of major elements in solution were measured by a multitype inductively coupled plasma (ICP) emission spectrometer (ICPE- 9000 SHIMADZU, Japan). Detection limits were on the order of  $50 \mu\text{g/L}$ . The error was estimated to be below  $5\%$ . Concentrations of As and Fe were measured using a Thermo Scientific™ ELEMENT 2™ and ELEMENT XR™ High Resolution (sector field) ICP-MS (Thermo Fisher Scientific, Bremen, Germany). Detection limits for both elements were in the order of  $0.5\text{-}1 \mu\text{g/L}$  and an estimated error to be below  $3\%$ . Sulfide, ferrous iron, and nitrite concentrations were determined spectrophotometrically on samples filtered through  $0.2 \mu\text{m}$  pore size filters using a UV-2501 PC spectrophotometer (Shimadzu, Japan). Fe(II) and Fe total concentrations measured with ICP-OES matched within  $10\%$ .

Arsenic speciation (As(III) and As(V)) was determined by HPLC/ICPMS (high-performance liquid chromatography with inductively coupled plasma mass spectrometry). A Perkin Elmer-Sciex Series 200 HPLC coupled to a Perkin Elmer-Sciex Elan DRC II ICPMS (Concord, Ontario, Canada) were employed. The detection limit for those measurements is  $0.1 \mu\text{g/L}$ , the error is estimated to be below  $3\%$ . Anion concentrations, with a detection limit of  $50 \mu\text{g/L}$  for all the elements studied and an error below of  $10\%$ , were analyzed by Ion Chromatography (DX-3000, Dionex). Nitrate and nitrite analysis of

the nitrate batch production experiments were carried out using a SmartChem Discrete Wet Chemistry Analyzer model 450. The detection limits for nitrate and nitrite were 0.5 mg/L and 0.05 mg/L, respectively. DOC was determined using a Shimadzu TOC-VCPH analyzer (Shimadzu Scientific Instruments, Kyoto, Japan). These measurements have a detection limit of 5 mg/L.

In all of the above-mentioned analyses, calibration with sets of standards was performed and the regression coefficients exceeded 0.999. Different dilutions were performed to ensure that the concentration of the samples was within the concentration range of the standards. To check the accuracy of the results, laboratory standards and control samples were analyzed every 5-10 samples. Blanks and duplicates were also analyzed with each batch of samples.

**Arsenic K-edge X-ray absorption spectroscopy.** Arsenic K-edge extended X-ray absorption fine structure (EXAFS) spectra were collected at 10 - 15 K in fluorescence detection mode at the 11-2 wiggler beamline at SSRL (California, USA) with a Si(220) double crystal monochromator. The monochromator was fully tuned; the beam was slit to  $500 \mu\text{m} \times 2 \text{ mm}$  and kept unfocused to limit photo-induced redox reaction. Data was recorded using a high throughput 100-element Ge array detector. Signal to noise ratio was optimized using sollers slits and Ge/Al filters. Incident energy was calibrated by setting to 11,947 eV the energy position of the main peak in the  $L_{\text{III}}$ -edge of a Au foil recorded in double-transmission mode, resulting in the  $\text{As}^{\text{V}}$ -O maximum absorption peak at 11,875 eV. To preserve anoxic conditions during data collection, the samples were transferred from a  $\text{N}_2$  anaerobic chamber to the liquid He cryostat for measurement in a liquid  $\text{N}_2$  bath. Due to the highly dilute As concentrations in the sediment samples, 4-12 scans were collected for each sample to get a reliable EXAFS signal up to  $k = 13 \text{ \AA}^{-1}$ . Scans were averaged, normalized and background subtracted using the Athena code<sup>6</sup>. Normalized spectra were

obtained by fitting a linear function to the pre-edge region and a power of two polynomial to the post-edge region. Data were background subtracted over the 0 - 13.4 Å<sup>-1</sup> *k*-range using the autobk algorithm. No clamps were fixed on the spline curve. Linear combination fitting (LCF) of XANES data was performed from -20 to 60 eV with E<sub>0</sub> set to 11,868 eV. LCF of EXAFS data were performed on *k*<sup>3</sup>-weighted EXAFS data over a *k*-range of 3-12 Å<sup>-1</sup> and E<sub>0</sub> was set up at 11,868 eV, using Athena code<sup>6</sup>. Fast Fourier transforms were plotted using a Kaiser-Bessel window with a Bessel weight of 2.5. As(V)-O, As(III)-O and As(III)-S local environments were respectively modeled by using As(V)-sorbed ferrihydrite, As(III)-sorbed ferrihydrite, glutathione-bound As(III) and arsenian pyrite. The identity of the model compounds and their spectra were previously reported<sup>7</sup>.

**Iron K-edge X-ray absorption spectroscopy.** Iron K-edge spectra on selected samples were collected in fluorescence and transmission detection mode in the XAFS beamline at ELETTRA (Trieste, Italy) and at the SSRL on BL 4-1 at 80K (at cryogenic temperature). The samples were diluted with fructose and prepared as pellets under N<sub>2</sub> atmosphere. Similarly as for As measurements, to preserve the anoxic conditions the sample was transferred to the beam line in a liquid N<sub>2</sub> bath. Data energy was calibrated by setting to 7,112 eV the energy position of the first inflection point in the edge of a Fe foil recorded in double transmission setup. Three-four scans averaged for each sample to an EXAFS signal up to *k* =10, *k*=11 and *k*=11.5 Å<sup>-1</sup> depending on the sample. The scans were averaged, normalized and background subtracted using the Athena code. No clamps were fixed on the spline curve. LCF of EXAFS data was performed on *k*<sup>3</sup>-weighted EXAFS and E<sub>0</sub> was set 7,125 eV, using Athena code<sup>6</sup>. Model compounds used for the LCF included siderite, biotite, illite, chlorite, goethite, and ferrihydrite.

**Sulfur K-edge X-ray absorption spectroscopy.** S-K-edge XANES spectra was collected at beamline 4-3 at SSRL using a double-crystal monochromator (Si [111] crystal). Samples

were thinly brushed on sulfur-free polyimide tape Kapton® tape mounted on aluminum sample holders and analyzed under a He atmosphere using a passivated implanted planar silicon (PIPS) fluorescence detector. The sample preparation was carried out inside the anaerobic glove box (5% H<sub>2</sub> : 95% N<sub>2</sub> atmosphere) and XANES data was collected under He atmosphere at ambient temperature. Four XANES spectra were collected for each sample. Scans were averaged in Sixpack<sup>8</sup>, normalized and background subtracted using the Athena code<sup>6</sup>. Energy was calibrated between each set of sample scans using the centroid of the first peak of sodium thiosulfate, assigned to 2472.02 eV. Sulfur XANES spectra were fit by linear least squares combination fits using reference compounds (pyrite, organic sulfur (S-cysteine), elemental sulfur and sulfate) and using Athena code<sup>6</sup>.



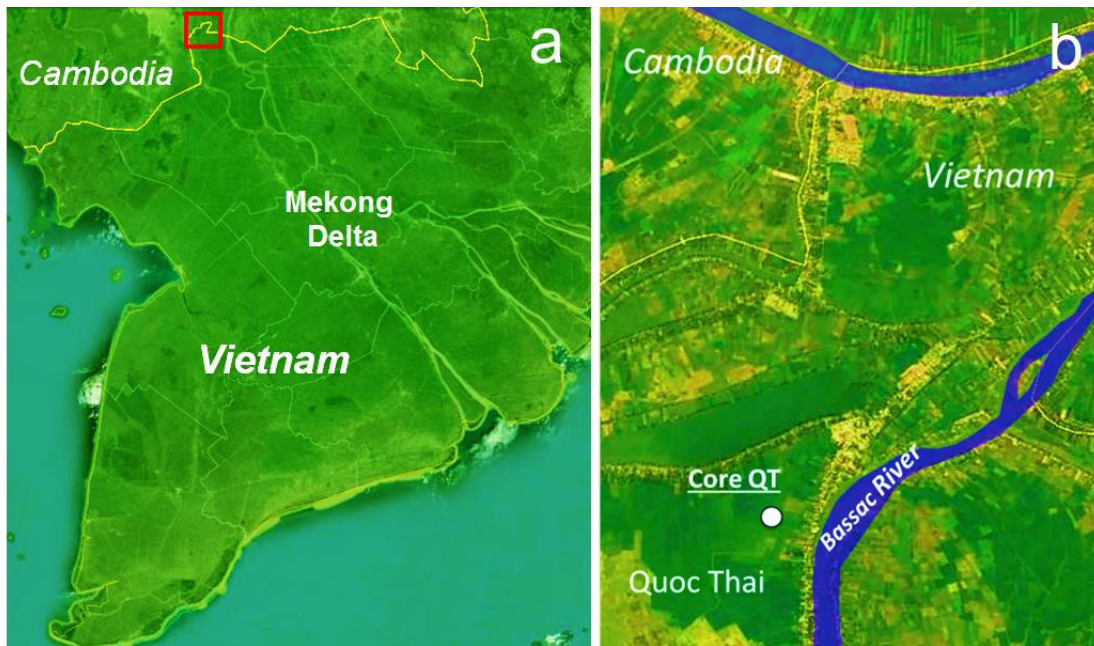


**Figure S1.** Location of the area of study. (a) A satellite image of South Vietnam and the Mekong Delta. The red rectangle shows the region in (b), which corresponds to a satellite image showing the sediment core sampling location (white dot; GDP coordinates:  $10^{\circ}54.329'$  N and  $105^{\circ}4.746'$  E; elevation: 3 m) in the Quoc Thai commune. The figures are modified from maps available at [www.google.com/maps](http://www.google.com/maps).

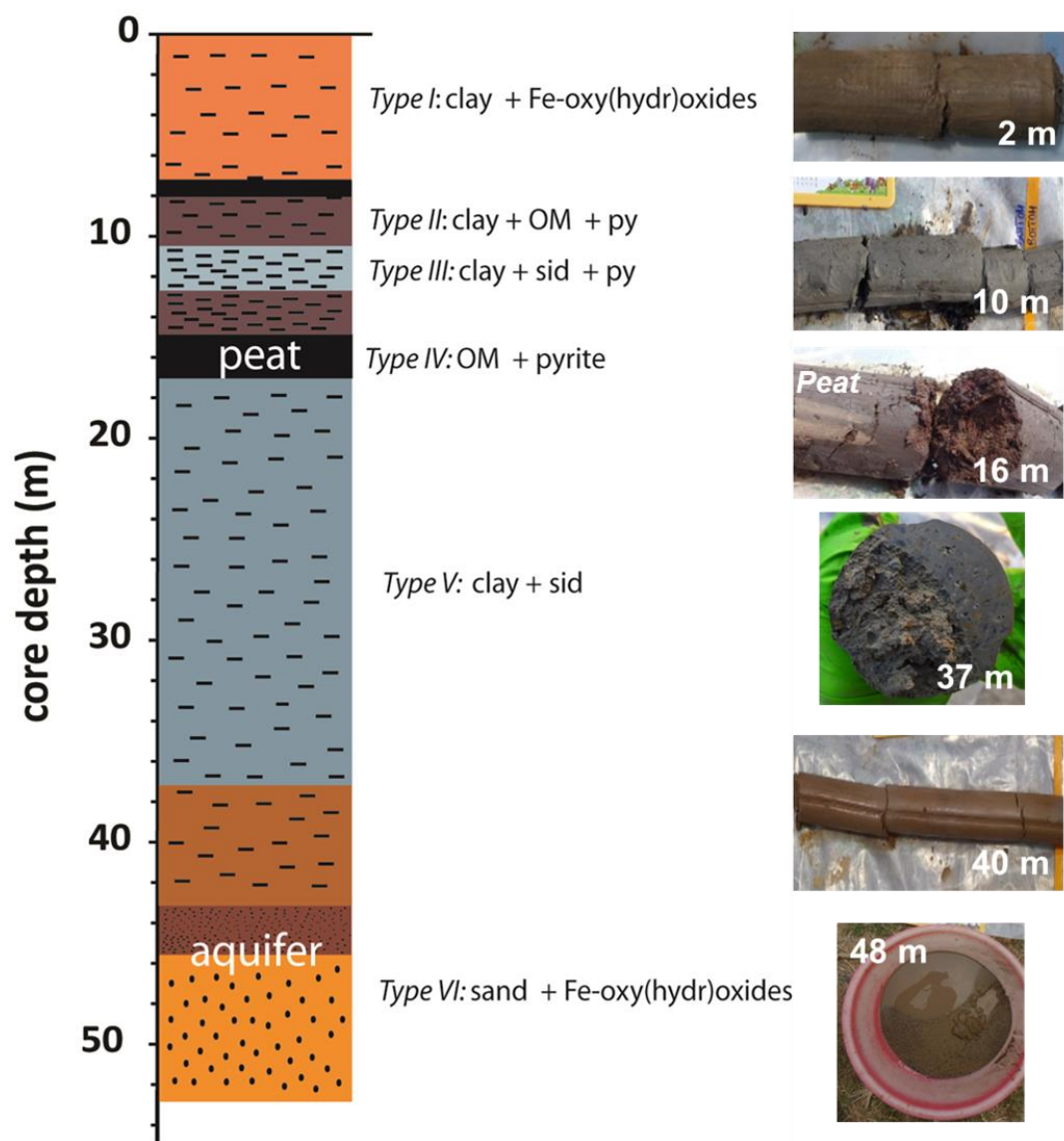


**Figure S2.** Scheme showing the lithology of the QTC-2, QTC-3 (from Wang et al.<sup>7</sup>) and QTC-5 cores and pictures of the sediments at various depths. In addition to the 5 layers identified in Wang et al.<sup>7</sup>, an additional layer (aquifer) was labeled type VI. Note: OM: organic matter; py: pyrite; sid: siderite.

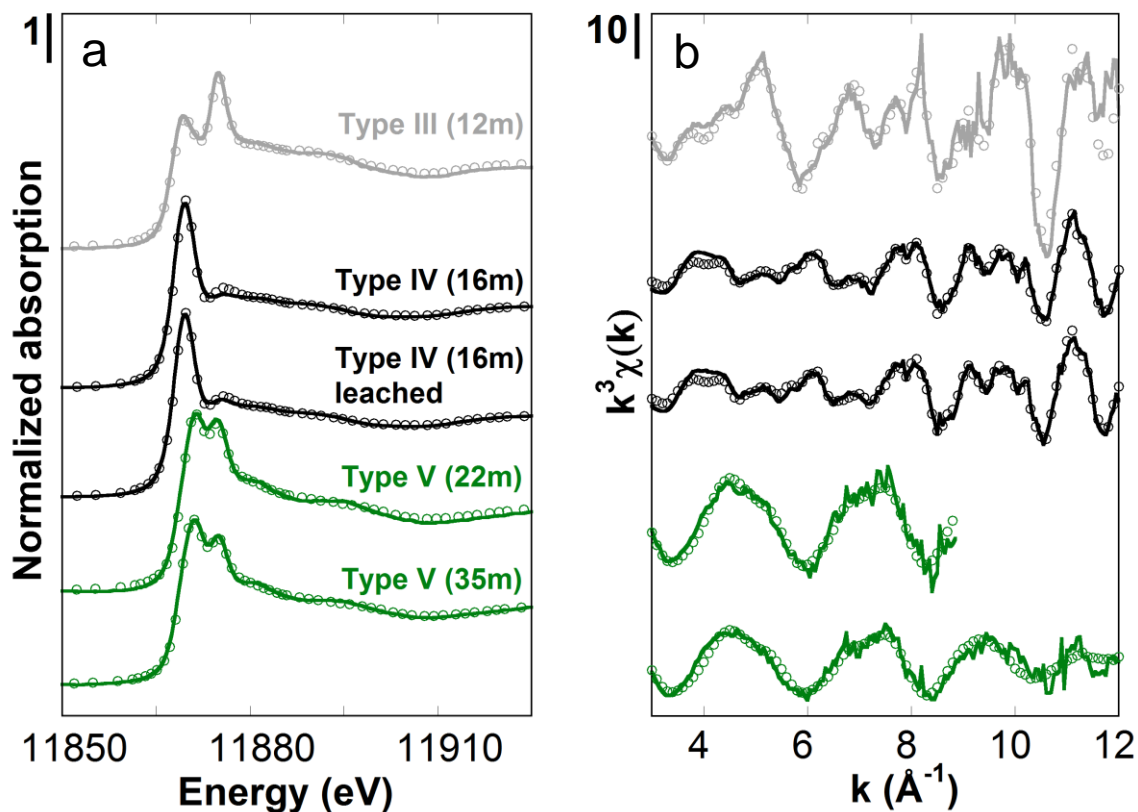


**Figure S3.** As K-edge XAS data. As K-edge XAS data collected at 10 K for selected QTC3 sediment samples and results of linear combination fit (LCF). Experimental and calculated curves are plotted as solid and dotted lines, respectively. XANES spectra (a) of sediment types III (12 m) showed two absorption peaks. The one at  $\sim 11,869$  eV corresponds to a mixture of As in arsenian pyrite (at 11,868.7 eV) and S-bound As(III) (at 11,869.5 eV),<sup>7</sup> while the one at  $\sim 11,875$  eV was assigned to O-bound As(V).<sup>7,9,10,11</sup> The spectrum of type IV organic-rich layer (16 m), before and after the leaching experiments performed with AGW, displayed a main absorption maximum at 11,869 eV resulting from a mixture of As in arsenian pyrite (at 11,868.7 eV) and S-bound As(III) (at 11,869.5 eV). The spectrum of sediment V (22 m and 35 m) showed two absorption peaks: one of O-bound As(III) at 11,871.4 eV.<sup>9,11,12</sup> and one of O-bound As(V) at 11,875 eV; (b) unfiltered EXAFS  $k^3\chi(k)$  functions in the  $k$  range of 3-12  $\text{\AA}^{-1}$ . The LCF results are reported in Table S4. Results of QTC3-35 m, indicated in grey, are from Wang et al.<sup>7</sup>

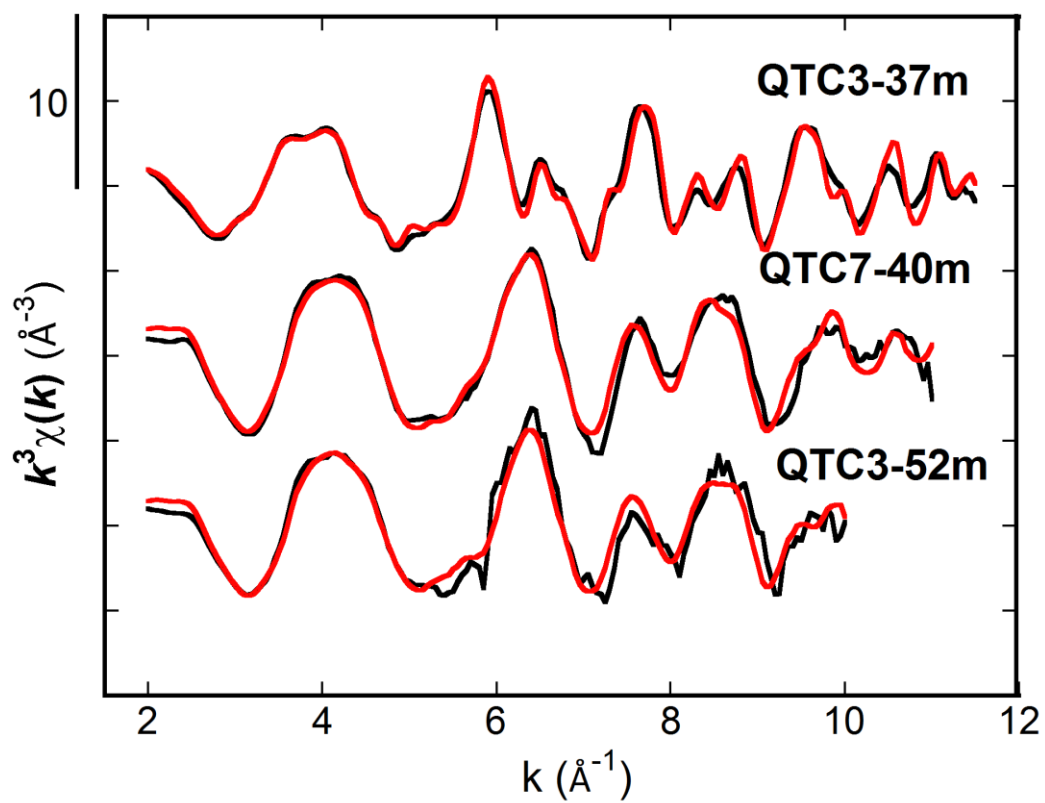


**Figure S4.** Fe K-edge EXAFS data (black) and linear combination fit (LCF) of Fe K-edge EXAFS data (red) for QT sediments: QTC3-37m, QTC7-40m and QTC3-52m (aquifer sediments).

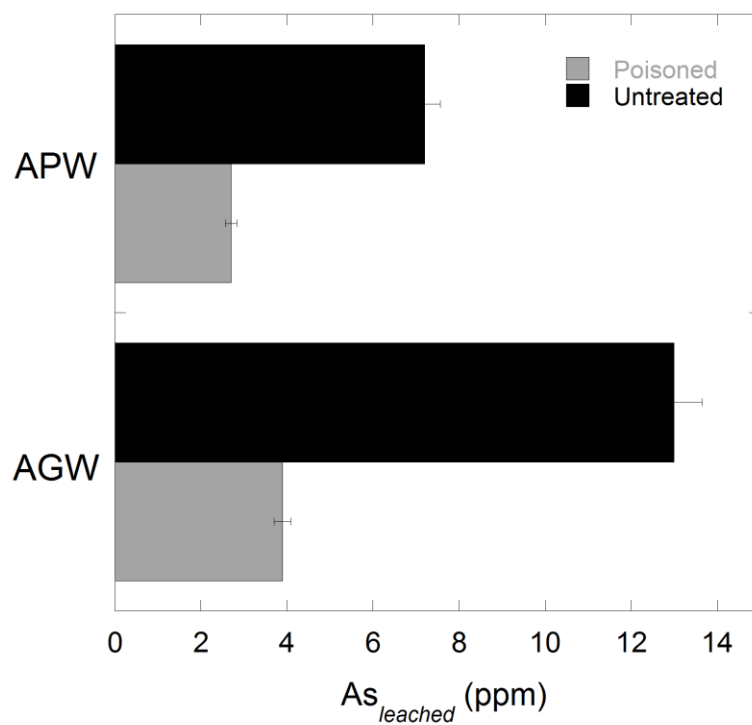


**Figure S5.** Arsenic leached after 600 h in leaching flow-through experiments performed with artificial porewater (APW) and artificial groundwater (AGW) and the peat layer (type-IV sediment layer) poisoned previously with NaN<sub>3</sub> (grey) and untreated (black).

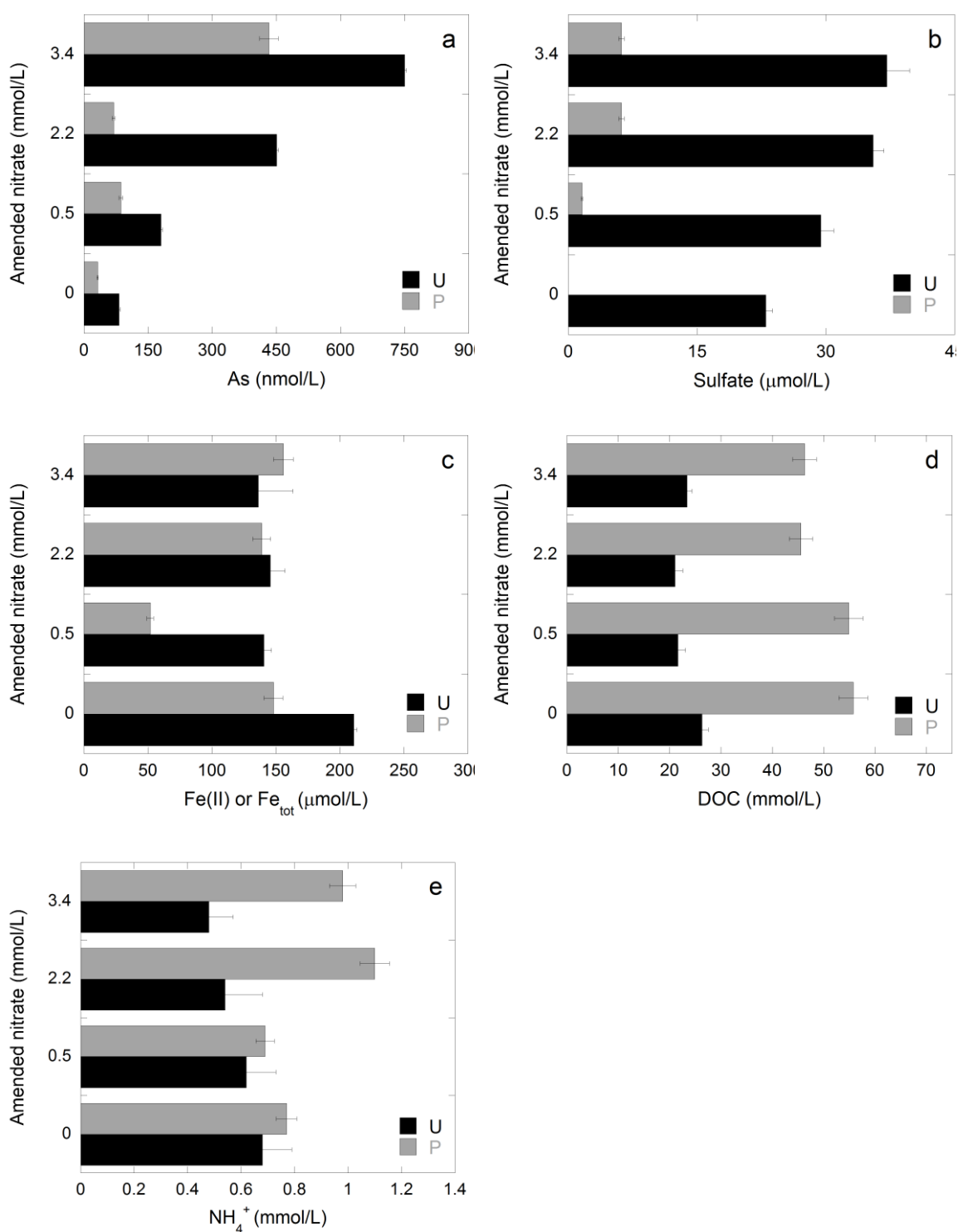


**Figure S6.** Comparison of the concentrations of As (a); sulfate (b); Fe(II) or Fe total (c); DOC (d) and  $\text{NH}_4^+$  (e) at the end of the batch experiments performed with the peat sediment (type-IV sediment layer) and APW-B versus the initial nitrate concentrations (0, 0.05, 0.5, 1, 2.2 and 3.4 mM) of sodium azide-treated experiments (P, grey bars) and untreated experiments (U, black bars). U values correspond to the average of the triplicate experiments.

**Table S1.** Experimental conditions and total As leached during 600 h in the flow-through leaching experiments.

Experiment	Depth (m)	Sediment type <sup>12</sup>	mass (g)	BET (m <sup>2</sup> /g)	As <sub>solid</sub> (ppm)	As <sub>leached</sub> (μg/m <sup>2</sup> )	As <sub>leached</sub> (μg/m <sup>2</sup> )	As(III) <sub>leached</sub> (%)	As(V) <sub>leached</sub> (%)	Input solution
QTC3-2A	2	Type I	4	19.5	21	1.0	0.05	76	24	AGW
QTC3-2B	2	Type I	4	19.5	21	1.4	0.07	73	27	
QTC3-12A	12	Type III	4	12.9	11	2.0	0.15	89	11	
QTC3-12B	12	Type III	4	12.9	11	1.1	0.08	95	5	
QTC3-14A	14	Type II	4	13.5	12	1.4	0.10	100	-	
QTC3-14B	14	Type II	4	13.5	12	1.6	0.12	100	-	
QTC3-Peat 1	16	Type IV	2	11.2	34	14.3	1.21	79	21	
QTC3-Peat 2	16	Type IV	2	11.2	34	11.7	0.99	77	23	
*QTC3-Peat 1-NaN <sub>3</sub>	16	Type IV	2	11.2	34	3.4	0.30	92	8	
*QTC3-Peat 2-NaN <sub>3</sub>	16	Type IV	2	11.2	34	4.4	0.40	93	7	
QTC3-22A	22	Type V	4	25.7	12	2.8	0.10	100	-	
QTC3-22B	22	Type V	4	25.7	12	3.3	0.13	100	-	
QTC3-37A	37	Type V	4	20.4	17	0.9	0.05	67	33	
QTC3-37B	37	Type V	4	20.4	17	0.7	0.03	55	45	
Aquifer 1	48	Type VI	4	1.4	7	0.3	0.24	78	22	
Aquifer 2	48	Type VI	4	1.4	7	0.3	0.22	71	29	
QTC3-Peat 3	16	Type IV	2	11.2	34	8.3	0.74	73	27	APW
QTC3-Peat 4	16	Type IV	2	11.2	34	6.0	0.54	78	22	
*QTC3-Peat 3-NaN <sub>3</sub>	16	Type IV	2	11.2	34	2.5	0.22	70	30	
*QTC3-Peat 4-NaN <sub>3</sub>	16	Type IV	2	11.2	34	2.9	0.26	85	15	

**AGW:** pH= 8.1; 1.5 mM of Ca, 0.8 mM of Mg, 0.05 mM of K, 5 mM of Na, 1.3 mM of NH<sub>4</sub>, 6.5 mM of Cl, 4 mM HCO<sub>3</sub><sup>-</sup>, 0.5 mM of NO<sub>2</sub><sup>-</sup>, 1 mM acetate

**APW:** pH= 7.5; 1.25 mM of Ca, 3.35 mM of Mg, 45.5 mM of Na, 3.5 mM of NH<sub>4</sub><sup>+</sup>, 57.6 mM of Cl, 3.8 mM HCO<sub>3</sub><sup>-</sup>, 0.03 mM of NO<sub>3</sub><sup>-</sup>, 0.5 mM acetate

\* Sediment was previously treated with sodium azide (NaN<sub>3</sub>)

**Table S2.** Composition of the peat layer porewater of QT-C5 core.

<b>Depth</b>	(m)	16			
<b>pH</b>					7.3
<b>Alkalinity</b>	(mmol/L)	4			
<b>(mmol/L)</b>	<b>TOC</b>	2.42	<b>(<math>\mu</math>mol/L)</b>	<b>Sr<sup>+2</sup></b>	7.30
	<b>NH<sub>4</sub><sup>+</sup></b>	3.44		<b>Mn<sup>+2</sup></b>	1.64
	<b>Cl<sup>-</sup></b>	56.4		<b>Ba<sup>+2</sup></b>	4.37
	<b>SO<sub>4</sub><sup>-2</sup></b>	0.09		<b>S(-II)</b>	2.06
	<b>NO<sub>3</sub><sup>-</sup></b>	0.03		<b>Fe(II)</b>	3.10
	<b>Ca<sup>2+</sup></b>	1.25		<b>As(III)</b>	0.81
	<b>K<sup>+</sup></b>	0.67		<b>As(V)</b>	0.03
	<b>Mg<sup>2+</sup></b>	3.33		<b>As<sub>tot</sub></b>	0.84
	<b>Na<sup>+</sup></b>	44.6			
	<b>Si<sup>4+</sup></b>	0.64			



**Table S3.** LCF results of the XANES and EXAFS data at As K-edge of QTC3 sediments. The percentage of As components is normalized to a sum of 100%. The fitting of the XANES or EXAFS signal was performed in the  $E$  range of 11,750 – 12,480 eV or the  $k$  range of 3 – 12 Å<sup>-1</sup>, respectively. Values within brackets indicate standard deviation in the last reported digit and correspond to 5 times the sigma values returned by the minimization routine. Actual uncertainties on the components are estimated to 20% or 10% of the reported fit values for the XANES or EXAFS signal, respectively. A dash (-) indicates that the component is either negligible or incompatible with the fitting. Results of QTC3-35 m, indicated in grey, are from Wang et al.<sup>7</sup>

Sample		As-Pyrite	As(III)-S	As(III)-O	As(V)-O	R-factor	Reduced Chi-sq
		%	%	%	%		
QTC3-12m	EXAFS	50 (13)	11 (10)	10 (10)	29 (13)	0.103	3.07
	XANES	37 (8)	19 (9)	17 (6)	27 (5)	0.001	0.0015
QTC3-16m	EXAFS	42 (4)	58 (6)	-	-	0.07	0.49
	XANES	30 (5)	70 (7)	-	-	0.0012	0.0014
QTC3-16m after flow- through	EXAFS	42 (4)	58 (6)	-	-	0.07	0.49
	XANES	32 (4)	68 (4)	-	-	0.0005	0.0006
QTC3-22m	EXAFS	-	18 (10)	50 (15)	31 (15)	0.063	0.887
	XANES	-	15 (4)	63 (5)	22 (5)	0.001	0.0018
QTC3-35m	EXAFS	-	21 (10)	47 (8)	31 (8)	0.1631	1.1
	XANES	-	27 (3)	54 (3)	19 (3)	0.000495	0.0006

**Table S4.** LCF results of the EXAFS data at Fe K-edge of the deepest QTC sediments. The percentage of Fe components is normalized to a sum of 100%. The fitting of EXAFS signal was performed in the  $k$  range of 2 – 11.5, 2-11 and 2-10 Å<sup>-1</sup>, for QTC3-37m, QTC7-40m, and QTC3-52m, respectively. Values within brackets indicate standard deviation in the last reported digit and correspond to 4 times the sigma values returned by the minimization routine. Actual uncertainties on the components are estimated to 10%. A dash (-) indicates that the component is either negligible or incompatible with the fitting.

Sample	siderite	biotite	Illite	chlorite	goethite	ferrihydrite	R-factor	Reduced Chi-sq
	%	%	%	%	%	%		
<b>QTC3-37m</b>	46 (4)	26 (8)	28 (6)	-	-	-	0.0265	0.00535
<b>QTC7-40m</b>	-	-	25 (16)	15 (10)	36 (13)	24 (20)	0.03904	0.01336
<b>QTC3-52m</b>	-	-	-	19 (10)	28(16)	53 (20)	0.0607	0.0205

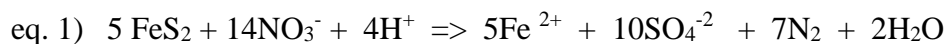
**Table S5.** Amount of arsenic released in the flow-through experiments performed with AGW from NOM and arsenian pyrite with respect to the initial concentration of As in the sediment (peat, type-IV sediment layer). The distribution of the species is based on the As EXAFS LCF results (Table S4). The fraction of As-S and As-pyrite was calculated based on the results of the LCF fit and the total amount of As determined by XRF or by subtraction of As released from the original amount of As. Measured values are in bold and calculated are not, and the LCF fitting-derived values are in italics.

Sample	Type of measurement	As in the solid			As released to solution	
		XRF	EXAFS		Total aqueous As	
		As <sub>total</sub>	As-S	As-Pyrite		
		ppm				
16 m peat	<i>Before reaction</i>	XRF	<b>34</b>	<i>19.9</i>	<i>14.1</i>	-
	<i>After reaction</i>	XRF	<b>20.8</b>	<i>12.0</i>	<i>8.8</i>	-
		Subtracting As released to solution	<i>19.7</i>	<i>11.4</i>	<i>8.3</i>	<b>14.3</b>

**Table S6.** LCF results of the XANES data at S K-edge for peat sediment samples before the reaction (pi) and after batch reaction with APW amended with 0, 1, 2.2 and 3.4 mM of nitrate (corresponding to p0, p1, p2, p3) for 40 days. Values within brackets indicate standard deviation in the last reported digit and correspond to 3 times the sigma values returned by the minimization routine. There are two different batches of peat prior to incubation (hence pi1 and pi2).

Sample	Pyrite	S-cysteine	Sulfate	R-factor	Reduced Chi-sq
	%	%	%	( $\times 10^{-4}$ )	( $\times 10^{-3}$ )
<i>pi1</i>	79 (3)	19 (3)	1 (1)	6.16	3.69
<i>pi2</i>	83 (3)	16 (3)	1 (1)	5.30	3.14
<i>p0</i>	67 (3)	30 (3)	2 (1)	9.56	5.71
<i>p1</i>	65(4)	33 (4)	2(2)	14.20	8.65
<i>p2</i>	68 (3)	30 (3)	3 (2)	8.93	5.26
<i>p3</i>	65 (3)	33 (4)	2 (2)	12.70	7.68

**Table S7.** Mass balance calculation of the pyrite oxidized by the amount of nitrate amended in the experiments and considering the following equations:



Amended nitrate	Pyrite potentially oxidized with amended nitrate	
	(eq. 1) <sup>13</sup>	(eq. 2) <sup>14</sup>
(μmol)		
85	30.4	121.4
55	19.6	78.6
25	8.9	35.7
12.5	4.5	17.9
1.25	0.4	1.8

For the calculations: the initial conditions obtained from the experimental conditions, the XRF and XANES results are: 1.5 grams of peat sediment, 25 mL of solution, 43.2 mg of sulfur and 530 μmol of pyrite in each experiment. Sulfur XANES results show pyrite dissolution in the range of 11-14% which correspond to 59 and 75 μmol of pyrite oxidized (which is less than what the amended nitrate can oxidize stoichiometrically according to eq. 1 and for the lower amended nitrate concentrations according to eq. 2). The amount of nitrate generated by ammonia oxidation (67.5 μmol) could oxidize 24.1 μmol of pyrite, which still does not account for all the pyrite oxidized (between 59 to 75 μmol).

## REFERENCES

- (1) Fernandez, A. M.; Sanchez-Ledesma, D. M.; Tournassat, C.; Melon, A.; Gaucher, E. C.; Astudillo, J.; Vinsot, A. Applying the Squeezing Technique to Highly Consolidated Clayrocks for Pore Water Characterisation: Lessons Learned from Experiments at the Mont Terri Rock Laboratory. *Appl. Geochemistry* **2014**, *49*, 2–21.
- (2) Entwisle, D.C., R. S. No Title. In *Geochemistry of Clay-Pore Fluid Interactions.*; Manning D.A.C., H. P. L. and H. C. R. (eds). C., Ed.; 1993; pp 365–388.
- (3) Peters, C.A., Yang, Y.C., Higgins, J.D., Burger, P.A., 1992. A Preliminary Study of the Chemistry of Pore Water Extracted from Tuff by One-- - dimensional Compression. In: Kharaka, Maest, (Eds.), *Water–Rock Interaction*, Pp. 741–745. **1992**, 1992.
- (4) Cline, J. D. Spectrophotometric Determination of Hydrogen Sulfide in Natural Waters. *Limnol. Ocean.* **1969**, *14*, 454–458.
- (5) Stookey, L. L. Ferrozine-A New Spectrophotometric Reagent for Iron. *Anal. Chem.* **1970**, *42* (7), 779–781.
- (6) Ravel, B., Newville, M. J. ATHENA, ARTEMIS, HEPHAESTUS: Data Analysis for X-Ray Absorption Spectroscopy Using IFEFFIT. *Synchrotron Radiat.* **2005**, *12*, 537–541.
- (7) Wang, Y.; Le Pape, P.; Morin, G.; Asta, M. P.; King, G.; Bártoová, B.; Suvorova, E.; Frutschi, M.; Ikogou, M.; Pham, V. H. C.; et al. Arsenic Speciation in Mekong Delta Sediments Depends on Their Depositional Environment. *Environ. Sci. Technol.* **2018**, *52* (6), 3431–3439.
- (8) Webb, S. M. SIXpack: A Graphical User Interface for XAS Analysis Using IFEFFIT. *Phys. Scr.* **2005**, *2005* (T115), 1011.
- (9) Wang, Y.; Morin, G.; Ona-Nguema, G.; Juillot, F.; Guyot, F.; Calas, G.; Brown, G. E. Evidence for Different Surface Speciation of Arsenite and Arsenate on Green Rust: An EXAFS and XANES Study. *Environ. Sci. Technol.* **2010**, *44* (1), 109–115.
- (10) Wang, Y.; Morin, G.; Ona-Nguema, G.; Juillot, F.; Calas, G.; Brown, G. E. Distinctive Arsenic(V) Trapping Modes by Magnetite Nanoparticles Induced by Different Sorption Processes. *Environ. Sci. Technol.* **2011**, *45* (17), 7258–7266.
- (11) Wang, Y.; Morin, G.; Ona-Nguema, G.; Brown, G. E. Arsenic(III) and Arsenic(V) Speciation during Transformation of Lepidocrocite to Magnetite. *Environ. Sci. Technol.* **2014**, *48* (24), 14282–14290.
- (12) Xie, X.; Ellis, A.; Wang, Y.; Xie, Z.; Duan, M.; Su, C. Geochemistry of Redox-Sensitive Elements and Sulfur Isotopes in the High Arsenic Groundwater System of Datong Basin, China. *Sci. Total Environ.* **2009**, *407* (12), 3823–3835.
- (13) Torrentó, C.; Cama, J.; Urmeneta, J.; Otero, N.; Soler, A. Denitrification of Groundwater with Pyrite and *Thiobacillus Denitrificans*. *Chem. Geol.* **2010**, *278* (1–2), 80–91.
- (14) Zhang, Y. C.; Slomp, C. P.; Broers, H. P.; Passier, H. F.; Cappellen, P. Van. Denitrification Coupled to Pyrite Oxidation and Changes in Groundwater

Quality in a Shallow Sandy Aquifer. *Geochim. Cosmochim. Acta* **2009**, 73 (22), 6716–6726.